A New Design Approach for Low Phase-Noise Reflection-Type MMIC Oscillators

Friedrich Lenk, *Member, IEEE*, Matthias Schott, *Student Member, IEEE*, Jochen Hilsenbeck, and Wolfgang Heinrich, *Senior Member, IEEE*

***Abstract*—In this paper, optimization of the loaded quality factor Q_L for reflection-type heterojunction bipolar transistor (HBT) oscillators is investigated. The main result is an optimum relation between the S-parameter phases at the three transistor ports. A new design strategy for this type of oscillator is proposed. The analysis is verified by comparing several Ka-band monolithic-microwave integrated-circuit oscillators in GaAs HBT technology with different resonators. The measured loaded Q_L values correspond to the measured phase noise of the circuits. At an oscillation frequency of 33 GHz, an excellent phase noise of −87 dBc/Hz at 100-kHz offset frequency is achieved over the whole tuning range.**

***Index Terms*—Heterojunction bipolar transistors (HBTs), microwave oscillators, monolithic-microwave integrated-circuit (MMIC) oscillators, quality (Q) factor, voltage-controlled oscillators (VCOs).**

I. Introduction

Low PHASE-NOISE oscillators are key components in each microwave system. One of the circuit concepts most commonly applied is that of the reflection oscillator. For this type, two ports of the active device are terminated by impedances in such a way that a negative resistance appears at the remaining port. There, a third impedance is connected to ground to adjust the oscillation frequency. In the following, these three impedances are referred to as external impedances. To ensure oscillation startup, the product of the reflection coefficients from the active and passive parts of the circuit must be larger than unity with zero phase. This product is denoted as an open-loop gain in the following.

In the case of monolithic microwave integrated circuits (MMICs), all three external impedances are comparable in magnitude and achievable quality (Q) factor. Moreover, the inner elements of the transistor influence the oscillation frequency and, obviously, they also contribute to the loaded Q factor (Q_L) of the oscillator. Therefore, it is not easy to identify the resonator of the circuit unambiguously and, thus, to determine Q_L. This complicates design for low phase noise, which, according to Leeson's well-known paper [1], should maximize Q_L of the oscillator.

Only few contributions on these MMIC-specific issues are available in the literature. Recently, Nallatamby *et al.* [2], [3] published a first approach to generalize Leeson's treatment to the typical MMIC situation. The purpose of this paper is to give a design strategy as to how the optimum Q_L for the reflection-type HBT oscillator can be achieved. First, we establish a closed-form solution to calculate the open-loop gain. The determination of the loaded Q_L for this oscillator type is already shown in [4].

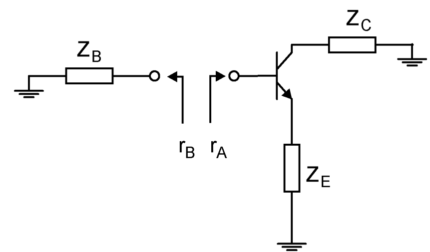

Fig. 1. Reflection-type oscillator.

In a second step, this approach is used to analyze the oscillator's properties as a function of the three external impedances. For this purpose, a new expression is introduced to qualify the external impedances.

The method is derived for a two-finger 3 × 30 μm^2 InGaP/GaAs HBT. Several MMIC oscillators with the same active part, but different resonating structures at the emitter port are analyzed to verify the method of loaded Q_L calculation. A voltage-controlled oscillator (VCO) with excellent phase noise [5] at 33 GHz is part of this comparison.

This paper is organized as follows. Section II presents the derivation and motivation of the open-loop gain and loaded-Q_L definition and its application to oscillator analysis. Section III introduces a new Q factor definition to characterize the external impedances, which are not operated in resonance. This definition is used in Section IV, where the results of the analysis are discussed. Finally, circuit design and measurements for several oscillators are treated in Section V.

II. Oscillation Condition

In Fig. 1, the principle of a reflection-type oscillator is shown. Each port of the active device is terminated by an external impedance to ground, denoted by Z_E, Z_B, and Z_C, respectively, in Fig. 1. These impedances describe the complete bias network, varactor, and also output load. To evaluate the small-signal oscillation condition, two different formulations can be used, which are: 1) the closed-loop gain S_v, which is investigated in [4] and 2) the so-called open-loop gain S_s,

Manuscript received April 21, 2004; revised July 16, 2004. This work was support by the German Ministry for Education and Research (BMBF) under Contract 01BM050.

The authors are with the Ferdinand-Braun-Institut für Höchstfrequenztechnik, 12489 Berlin, Germany

Digital Object Identifier 10.1109/TMTT.2004.837319

formed by the product of two reflection coefficients after splitting the circuit into two subcircuits. In the following, according to Fig. 1, the base of the transistor is used as the split point and the open-loop gain S_s is derived as

$$r_B r_A = S_s. \tag{1}$$

This formulation is well known and can be determined by means of an oscillator test-port element in the commercial circuit simulators. Using 50 Ω as the reference impedance, a value of $S_s = 1.2 \ldots 1.4$ with zero phase is generally recommended to ensure oscillation startup.

The closed-loop gain S_v is needed to determine the loaded Q_L of the circuit, as shown in [4], but no empirical formula is present for the magnitude of this parameter. Moreover, practical circuit design is rather based on the open-loop gain according to (1). Therefore, we will include the open-loop gain in the following considerations and solve (1) for the external impedances.

First, the reflection coefficients r_A at the base (see Fig. 1) and r_B are calculated. With the admittance parameters of the transistor Y_a in grounded common-emitter configuration and Z_0 as reference impedance, one has

$$\begin{aligned} r_A &= \frac{Z_A - Z_0}{Z_A + Z_0} \\ r_B &= \frac{Z_B - Z_0}{Z_B + Z_0} \end{aligned} \tag{2}$$

with

$$\begin{aligned} Z_A &= \frac{1 + Y_{a22} Z_C + \left(\sum Y_a + |Y_a| Z_C\right) Z_E}{Y_{a11} + |Y_a|(Z_C + Z_E)} \\ |Y_a| &= Y_{a11} Y_{a22} - Y_{a12} Y_{a21} \\ \sum Y_a &= Y_{a11} + Y_{a12} + Y_{a21} + Y_{a22}. \end{aligned}$$

Now the results for r_A and r_B in (2) are inserted in (1), which yields

$$S_s = \frac{(Z_0 - Z_B)(Z_1 - Z_2)}{(Z_0 + Z_B)(Z_1 + Z_2)} \tag{3}$$

with

$$\begin{aligned} Z_1 &= Y_{a11} Z_0 + |Y_a| Z_0 (Z_C + Z_E) \\ Z_2 &= 1 + Y_{a22} Z_C + Z_E \left(|Y_a| Z_C + \sum Y_a\right). \end{aligned}$$

This formulation for the open-loop gain S_s corresponds to the closed-loop gain S_v in [4, eq. (7)].

The small-signal oscillation condition in (3) is satisfied for

$$S_s = |S_s| e^{j0} \text{ with } |S_s| > 1. \tag{4}$$

With magnitudes and phases of the three external impedances and the open-loop gain magnitude $|S_s|$, (3) and (4) involve a total of seven unknowns. To reduce this number, the following consideration is useful. At microwave frequencies, the three external impedances Z_B, Z_C, and Z_E are better described in terms of their reflection coefficients r_B, r_C, and r_E, respectively [see, e.g., r_B in (2)].

For MMIC oscillators, these reflection coefficients are commonly established by transformations using lines, capacitors, or inductors starting from the RF ground (which can also be formed by blocking capacitors). Since the resulting networks consist of low-loss reactive elements, the three reflection coefficients are comparable in magnitude and close to $|r| = 1$. This circumstance is used to reduce the number of variables in (3) and (4) assuming

$$|r_E| = |r_B| = |r_C| = |r_i|. \tag{5}$$

The three external impedances are now described by

$$r_B = |r_i| e^{j\varphi_B} \quad r_C = |r_i| e^{j\varphi_C} \quad r_E = |r_i| e^{j\varphi_E}. \tag{6}$$

Thus, five unknowns remain in (3) and (4), which are the three phases: 1) φ_B; 2) φ_C; and 3) φ_E; 4) the magnitude of the open-loop gain $|S_s|$; and 5) the magnitude of the reflection coefficient of the external impedances $|r_i|$. The phase of the emitter reflection-coefficient φ_E is treated as an independent variable. With $|r_i|$ and $|S_s|$ as parameters, the phase of the base and collector reflection coefficients φ_B and φ_C are then used to fulfill the oscillation condition represented by (3) and (4). For each emitter phase φ_E, one obtains a set of two solutions for base and collector phases φ_B and φ_C.

In a final step, (3) is rewritten for $Z_B = f(Z_C)$, which gives

$$Z_B = b_0 \frac{Z_C + b_1}{Z_C - b_2} \tag{7}$$

with

$$\begin{aligned} b_0 &= -Z_0 \frac{(|S_s| - 1)(|Y_a| Z_0) + (|S_s| + 1) Y_z}{(|S_s| + 1)(|Y_a| Z_0) + (|S_s| - 1) Y_z} \\ b_1 &= \frac{(|S_s| + 1)(1 + Z_E \sum Ya) + Z_0 (|S_s| - 1) Y_x}{(|S_s| - 1)(|Y_a| Z_0) + (|S_s| + 1) Y_z} \\ b_2 &= -\frac{(|S_s| - 1)(1 + Z_E \sum Ya) + Z_0 (|S_s| + 1) Y_x}{(|S_s| + 1)(|Y_a| Z_0) + (|S_s| - 1) Y_z} \\ Y_x &= Y_{a11} + |Y_a| Z_E \\ Y_z &= Y_{a22} + |Y_a| Z_E. \end{aligned}$$

This formulation of Z_B corresponds to [4, eq. (13)]. Hence, all of the following mathematics for the closed-loop gain S_v in [4] can be adopted to the open-loop gain S_s from (7), only the expressions for b_0, b_1, and b_2 have to be updated with the ones of (7).

Before the design procedure is described, however, some considerations on the Q factor of the (passive) external impedances are necessary.

III. Unloaded Q_U of External Impedances

When calculating the loaded Q_L of a reflection-type oscillator, as done in [4], a phase slope (in S-parameters) is attributed to each of the external impedances as a measure for the relevant effective Q factor. To avoid confusion regarding the phase term, we use for Y-parameters the expression φ_y and for S-parameters φ_s in the following.

For a simple *RLC* parallel resonator, the unloaded Q_U can be calculated in Y- parameters by

$$Q_U = \frac{\omega}{2}\left|\frac{d\varphi_y}{d\omega}\right|_{\omega\to\omega_0}. \tag{8}$$

This definition is only valid at the resonance frequency ω_0, where the phase of the resonator is $-\pi$ in terms of the reflection coefficient. In oscillator design, however, this physical definition of the Q factor does not provide all the information one is interested in. For example, in most cases, the networks at the three ports do not satisfy the resonance condition individually, i.e., the phases of the external impedances are not equal to $-\pi$, but may have arbitrary values. Hence, for oscillator analysis, a modified quantity needs to be defined, which is adapted to the requirements of oscillator design rather than based on the well-known Q-factor definition. One important feature is that it should hold at arbitrary phases and frequencies, and not only at resonance. This new quantity will be denoted by Q'_U in the following.

Let us consider a resonator in terms of S-parameters, i.e., described by its input reflection factor r. For a first-order approximation close to the frequency of resonance, a lossless transmission line connected to the resonator then adds a constant phase shift only as follows:

$$r(l) = r(0)e^{-j2\beta l}. \tag{9}$$

Consequently, the quantities important for oscillator phase noise, namely, phase slope and magnitude $|r|$, remain unchanged. Therefore, if we define the new quantity Q'_U such that it is based on phase and magnitude of the reflection factor r instead of admittance Y or impedance Z, this formulation also should provide a reasonable value for phases other than $-\pi$.

To define Q'_U in this way, a parallel resonator is used as a reference. It is characterized by the conductance G, representing the loss, the inductance L, and the frequency of resonance $\omega_0 = 1/\sqrt{L\cdot C}$.

The reflection coefficient r of the parallel resonator reads

$$r = \frac{\omega_0^2 - \omega^2 + j\omega L\omega_0^2\,(G - Y_0)}{\omega^2 - \omega_0^2 - j\omega L\omega_0^2\,(G + Y_0)}. \tag{10}$$

At the frequency of resonance ω_0, phase slope and magnitude of r are

$$\left.\frac{d\varphi_s}{d\omega}\right|_{\omega\to\omega_0} = \frac{4Y_0}{L\omega_0^2\,(G^2-Y_0^2)} \qquad |r|\big|_{\omega\to\omega_0} = \frac{Y_0-G}{Y_0+G}. \tag{11}$$

Applying the conventional Q-factor definition of (8) (based on the admittance), one obtains

$$Q_U = \frac{\omega}{2}\left|\frac{d\varphi_y}{d\omega}\right| = \frac{1}{\omega_0 LG}. \tag{12}$$

Solving (11) for G and L and insertion in (12) yields an expression for Q'_U in terms of $|r|$ and φ_s, which is independent of reference admittance Y_0

$$Q'_U = \left.\frac{-|r|\omega\dfrac{d\varphi_s}{d\omega}}{1-|r|^2}\right|_{\omega\to\omega_0}. \tag{13}$$

The sign in the numerator can be defined arbitrarily. We choose the negative sign in order to achieve positive values for Q'_U for negative phase slope $d\varphi_s/d\omega$. For oscillator design, only the magnitude $|Q'_U|$ is of interest. This quantity $|Q'_U|$ has the advantage over the conventional Q_U formulation that its value does not vary significantly when connecting a low-loss transmission line to the resonator since $|r|$ and $|d\varphi_s/d\omega|$ then remain almost unchanged.

IV. Design Considerations

To investigate the loaded Q_L of the oscillator, it is useful to add a phase slope to each of the external impedances (see [4]). Now, with the newly defined Q'_U from (13), this phase slope can be replaced by

$$\frac{d\varphi}{d\omega} = -\frac{Q'_U\left(1-|r_i|^2\right)}{|r_i|\omega_0}. \tag{14}$$

Solving the open-loop gain according to (3) and (4), one obtains, for instance, a phase φ_{B0} at the base. Adding a phase slope there can be formulated as follows (which corresponds to [4, eq. (11)]):

$$\begin{aligned} r_B &= |r_i|e^{j\left(\varphi_{B0}+(\omega-\omega_0)\,\frac{d\varphi}{d\omega}\big|_{\omega\to\omega_0}\right)} \\ &= |r_i|e^{j\left(\varphi_{B0}-\left(\frac{\omega}{\omega_0}-1\right)\frac{Q'_{UB}\left(1-|r_i|^2\right)}{|r_i|}\right)}. \end{aligned} \tag{15}$$

In this way, the loaded Q_L of the oscillator can be calculated as a function of the Q'_U values of the three external impedances for arbitrary phase values at the ports. The procedure can be summarized as follows.

- Step 1) Evaluate the admittance parameters Y_a of the active device at the desired frequency.
- Step 2) Fix the magnitude of the reflection coefficients of the three external impedances $|r_i|$ and the desired magnitude of the open-loop gain $|S_s|$ (e.g., 1.2 for 50-Ω reference impedance).
- Step 3) For a given emitter phase φ_E, calculate the corresponding set of base and collector phases $\varphi_{B1,2}$ and $\varphi_{C1,2}$ with b_0, b_1, and b_2 from (7) and [4] [(15) and (16)].
- Step 4) Add a phase slope to each reflection coefficient (in analogy to what is shown in (15) for the base).
- Step 5) Calculate the loaded Q_L of the oscillator.

Steps 3)–5) needs to be carried out for each emitter phase in the range $\varphi_E = 0\ldots 2\pi$.

As an example, the performance of a reflection-type oscillator at 38 GHz with a two-finger 3×30 μm^2 GaInP–GaAs HBT as an active device is presented here. The small-signal equivalent circuit according to [6] is used to describe the HBT. We assume $|r_i| = 0.95$ for the magnitude of the reflection coefficients of the three external impedances and $|S_s| = 1.2$ for the open-loop gain. In Fig. 2, the results for $\varphi_{B1,2}$ and $\varphi_{C1,2}$ as a function of the emitter phase φ_E are shown. Now Steps 1)–3) of the above-described procedure are performed.

For Step 4), three different cases are considered. In the first case, the base reflection coefficient is expanded by a phase-slope

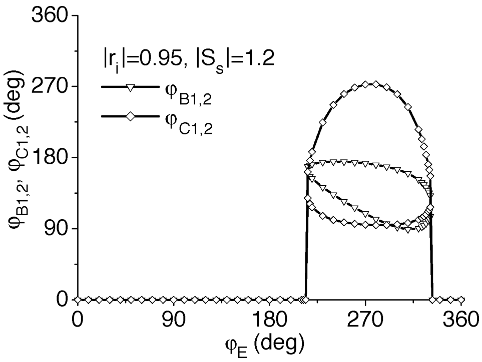

Fig. 2. Calculated base and collector phases $\varphi_{B1,2}$ and $\varphi_{C1,2}$ in dependence to the emitter phase φ_E.

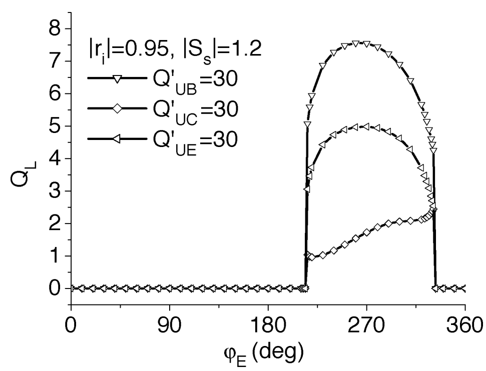

Fig. 3. Loaded Q_L of a 38-GHz reflection-type oscillator against emitter phase, for increased phase slope at the base, collector, and emitter, respectively.

term with $Q'_{UB} = 30$ according to (15). φ_E and φ_C are assumed to be constant with frequency in the vicinity of the oscillation frequency and, thus, do not contribute to the Q_L of the oscillator. For this configuration, oscillator Q_L is determined taking into account the inner elements of the HBT and the phase slope associated with the base impedance.

In the second and third cases, this simulation is repeated adding the phase-slope term to the collector and emitter, respectively, while keeping the other two impedances frequency independent in the vicinity of the oscillation frequency.

In Fig. 3, the results are plotted. For each emitter phase value, the solution pair φ_{Bi} and φ_{Ci} with the larger Q_L is used. For emitter-phase values $-27° < \varphi_E < 214°$, oscillation is impossible and the calculated Q_L is set to zero.

As one can see, the three external impedances do not influence Q_L equally. The Q'_U value at the base has the greatest impact on oscillator Q_L. Moreover, with comparable conditions at the three HBT ports, maximum Q_L (and, hence, lowest phase noise) is achieved for an emitter phase of $\varphi_E = 260°$. The corresponding phases at base and collector are $\varphi_B = 117°$ and $\varphi_C = -91°$.

An equal result is obtained when using negative values for the unloaded Q'_U in this procedure. Although the absolute values are not the same (in our case, one achieves lower values), the shapes of the curves remain unchanged. With increasing $|Q'_U|$, the deviations between the results for both signs vanish. Q_L is then dominated by Q'_U of the particular external impedance and, therefore, the influence of the active device is negligible.

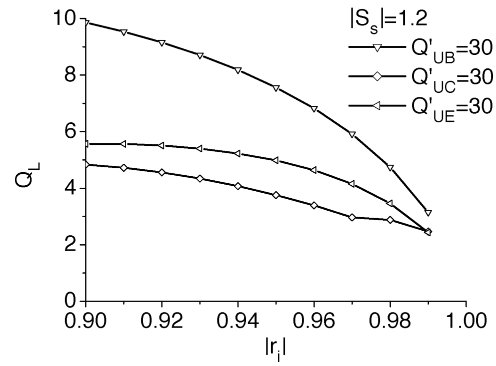

Fig. 4. Maximum Q_L of a 38-GHz reflection-type oscillator as a function of the magnitude $|r_i|$ of the external impedances for an unloaded Q'_U of 30 at the base, collector, and emitter, respectively.

In a second simulation, the effect of the magnitude $|r_i|$ of the external impedances is studied. For this purpose, we only consider the maximum of the curves in Fig. 3 and plot these values as a function of $|r_i|$. Fig. 4 presents the results. Varying collector and emitter magnitude, the resulting changes in Q_L are small. The magnitude value at the base is more critical. Thus, loss in the base network should be kept particularly small. This sensitivity corresponds to the curves in Fig. 3, where the base branch exhibits the greatest influence.

V. Experimental Verification

To validate the new design approach, a set of four MMIC oscillators (three fixed-frequency and one VCO [5]) in the Ka-band was realized using the Ferdinand-Braun-Institut für Höchstfrequenztechnik (FBH), Berlin, Germany, GaAs-HBT process [7], [8]. They are based on the reflection-type structure, but in contrast to Fig. 1, the emitter port of the transistor is used as the split point. Thus, the active part of the circuit consists of Z_B, Z_C, and the HBT, the passive part of the circuit, is formed by the emitter impedance Z_E.

In a first step, the active part was designed. To ensure consistency, the same active part is used for all four oscillators. Fig. 5 shows a chip photograph of the VCO. A series of two grounded metal–insulator–metal (MIM) capacitors and a coplanar waveguide (CPW) short stub are employed to transform a small inductance to the base port of the HBT. Nearly the same condition is required at the collector side, but because of the parallel output, a combination of spiral inductor and a $\lambda/4$ CPW are applied instead of a blocking capacitance. The output branch contains a coupling capacitance and a 10-dB attenuator. This was introduced in order to reduce load–pull effects during on-wafer measurements. A spiral inductor at the upper emitter side is used as an $\lambda/4$ line for dc ground connection.

To achieve higher $|Q'_U|$ in the passive part of the oscillators, coplanar lines with cross sections scaled by a factor of three are used. Series and parallel MIM capacitors adjust phase slope and magnitude. The circuit and element values are shown in Fig. 6 and Table I, respectively.

After circuit fabrication, the following measurements were performed.

- Oscillation frequency, output power, and phase noise were measured by means of an Agilent E5504 phase-noise system using the delay-line method.

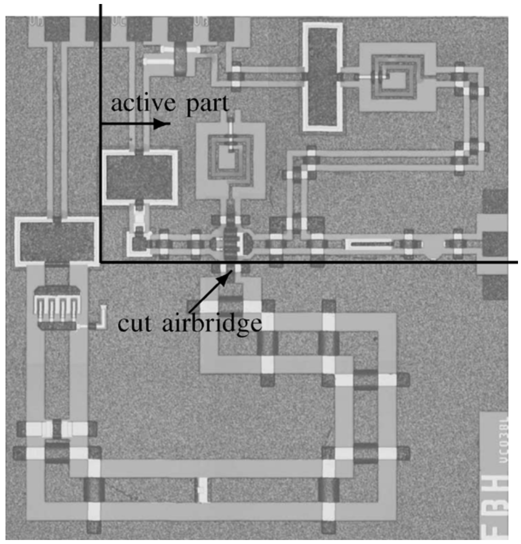

Fig. 5. Chip photograph of the Ka-band VCO. The active part (the same for all four oscillators) is separated by the solid line. Cutting the indicated air-bridge, active and passive part can be measured separately. Chip size is 1.2×1.3 mm^2.

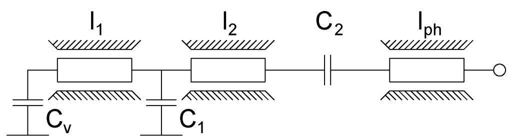

Fig. 6. Emitter circuit of the oscillators.

TABLE I
ELEMENT VALUES OF THE EMITTER CIRCUITS (SEE FIG. 6)

	C_v (fF)	l_1 (μm)	C_1 (fF)	l_2 (μm)	C_2 (fF)	l_{ph} (μm)
OSC0	300	1220			1080	
OSC1	300	68.5	1040	561	50	121
OSC2	300	59.0	800	519	50	690
VCO	$= f(V_d)$	175	490	479	75	1230

- For a single HBT, S-parameter measurements were performed at comparable bias points.
- By cutting an air-bridge (see Fig. 5), the circuits are divided into an active and passive part and S-parameter measurements were performed for both.

In Fig. 7, the simulation of the active part applying the measured HBT data is shown. Good agreement between measurements and simulation is obtained, which validates accuracy of the simulation tools. Oscillation is possible where $|r_a| > 1$, i.e., between 23.0–40.2 GHz.

In order to verify the Q_L formulation presented in [4], the loop gain S_v according to [4, eq. (5)] has to be investigated. For this purpose, an S-parameter simulation for the active and passive parts was performed and linked.

- The HBT is described by the measurement data in comparable bias points. The measured S parameters are transformed into Y-parameter Y_a.
- The passive circuits at each of the three transistor ports (base, collector, and emitter) are simulated. The reflection coefficients are transformed to Z_b, Z_c, and Z_e, respectively. For Z_e directly, the measurements of the passive part are used.

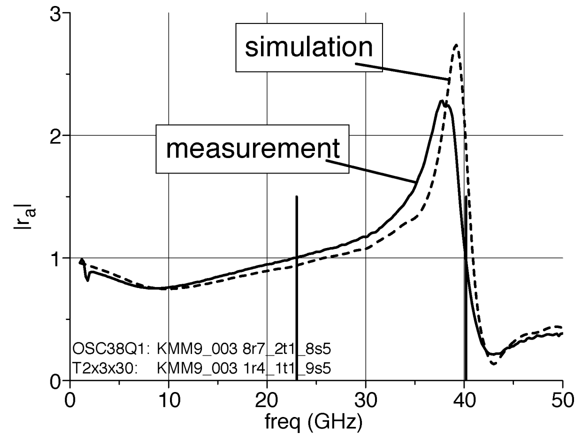

Fig. 7. Resimulation of the magnitude $|r_a|$ of the active part of the oscillators. Vertical lines indicate $|r_a| > 1$.

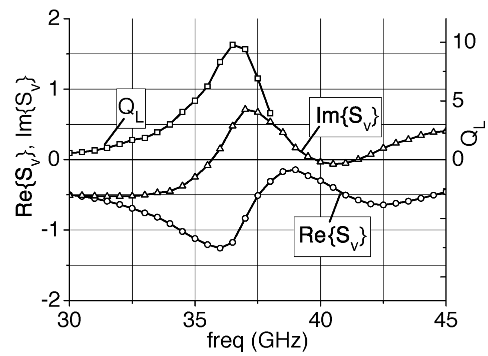

Fig. 8. Loop gain S_v and loaded Q_L for the Ka-band VCO. Tuning voltage is $V_d = 0$ V.

TABLE II
SIMULATION AND MEASUREMENT DATA OF THE Ka-BAND OSCILLATORS UNDER INVESTIGATION (THREE FIXED FREQUENCY AND ONE VCO). PHASE NOISE L_{SSB} REFERS TO AN OFFSET FREQUENCY OF 1 MHz

type	calculation using (16)				measurement	
	f_{osc} (GHz)	$\lvert S_v \rvert$	Q_L	L_{SSB} (dBc/Hz)	f_{osc} (GHz)	L_{SSB} (dBc/Hz)
OSC0	34.9	-1.30	5.48	-104.6	32.8	-103.7
OSC1	39.6	-1.24	4.58	-102.0	39.0	-101.4
OSC2	38.4	-1.32	7.44	-106.5	37.7	-107.0
VCO	35.7	-1.24	6.96	-106.5	34.2	-107.5

The loop gain was calculated according to the method from [4]. In Fig. 8, the results for the VCO with a tuning voltage of $V_d = 0$ V are plotted. From $\mathrm{Im}\{S_v\} = 0$, the frequency of oscillation f_{osc} can be determined. Corresponding plots are obtained for the three fixed-frequency oscillators $\mathrm{OSC0}, \ldots, \mathrm{OSC2}$. The data for all oscillators is collected in Table II. Besides the frequency of oscillation f_{osc}, the $|S_v| = \mathrm{Re}\{S_v\}$ and Q_L values at this frequency are listed.

The loaded Q_L of the different oscillators varies from 4.58 to 6.96. Leeson's formula [1] does not allow to predict the phase noise because the noise parameters of the active circuit are not

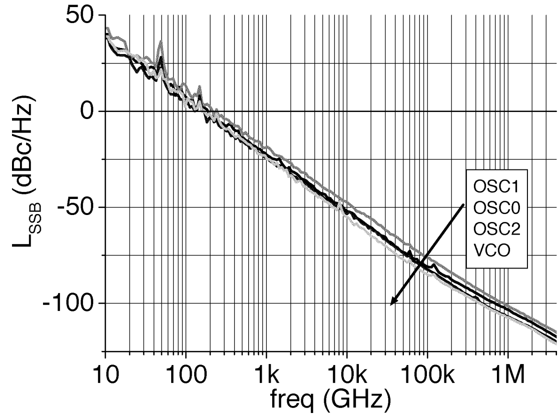

Fig. 9. Measured phase noise of the four oscillators as a function of offset frequency.

known *a priori*. However, since all four oscillators contain the same active configuration and are operated at the same bias conditions, Leeson's formula provides a good means to compare the circuits (taking into account the differences in oscillation frequency $f_{\rm osc}$ and loaded Q_L). The output was realized at the collector using a narrow-band transformation network to the 50-Ω load. Since the resonant frequencies are different, the measured output power is not proportional to the internal power of the oscillator $P_{\rm out}$ from Leeson's formula. Therefore, in the following, a constant $P_{\rm out}$ is assumed for all of the circuits.

Applying

$$L_{\rm SSB}(f_a) = 10\log\left[\frac{2kT}{P_{\rm out}}\left(\frac{1}{2f_a}\right)^2\right] + 20\log\left[\frac{f_{\rm osc}}{Q_L}\right]$$
$$= -300.7\ {\rm dBc/Hz} + 20\log\left[\frac{f_{\rm osc}}{Q_L}\right] \qquad (16)$$

to the measurements of Q_L and $f_{\rm osc}$, the phase noise values in Table II denoted by "calculation" are extracted. The constant of −300.7 dBc/Hz is determined by fitting for an offset frequency f_a of 1 MHz based on the assumption of identical active circuits.

In Fig. 9, the measured phase-noise data is shown. The behavior of the oscillators is quite similar. With growing offset frequency, at approximately 200 kHz, the slope changes from −30 to −20 dB/dec. At an offset frequency of 1 MHz, therefore, the phase noise is dominated by the loaded Q_L of the circuit. Hence, this frequency (and not the 100-kHz data) is used when comparing simulation and measured phase noise data in Table II. Good agreement is achieved with errors below 1 dB. The simulated frequency of oscillation is slightly higher than the measured one. This is due to the transition from small- to large-signal operation when oscillation reaches its steady state.

For the design, simplified models for the discontinuities of the wide CPW lines were employed. Therefore, up to 8% error in frequency is observed, although all circuits were designed to oscillate at 38 GHz. Note that Table II collects the values at comparable bias points of the different oscillators, while the bias point of the VCO for minimum phase noise is slightly different.

VI. Conclusions

A new approach for optimizing low phase-noise reflection-type oscillators has been presented. It is especially suited for MMIC oscillators, where high-Q resonators are not available and, therefore, the inner elements of the active device have a great impact on the loaded Q_L of the circuit. The approach combines the investigation and optimization for the loaded Q_L introduced in [4] with the usual reflection-type oscillator design by means of the open-loop gain. By determining an optimum phase condition for the three impedances connected to the ports of the active device, it provides a possibility to take maximum advantage of the element Q factors with respect to phase noise.

A set of four comparable oscillators has been designed to confirm the presented Q_L calculation and its translation into phase noise. The VCO [5], which is the best of these four oscillators, has achieved an excellent phase noise of −87 dBc/Hz at 100-kHz offset frequency at 33-GHz oscillation frequency. The output power of this circuit is 4±0.5 dBm in the entire tuning range.

Acknowledgment

The authors would like to thank S. Schultz, FBH, Berlin, Germany, for performing the measurements.

References

[1] D. B. Leeson, "A simple model of feedback oscillator noise spectrum," *Proc. IEEE*, vol. 54, pp. 329–330, Feb. 1966.

[2] J.-C. Nallatamby, M. Prigent, M. Camiade, and J. Obregon, "Phase noise in oscillators—Leeson formula revisited," *IEEE Trans. Microwave Theory Tech.*, vol. 51, pp. 1386–1394, Apr. 2003.

[3] ——, "Extension of the Leeson formula to phase noise calculation in transistor oscillators with complex tanks," *IEEE Trans. Microwave Theory Tech.*, vol. 51, pp. 690–696, Mar. 2003.

[4] F. Lenk, M. Schott, J. Hilsenbeck, and W. Heinrich, "Optimizing MMIC reflection-type oscillators," in *IEEE MTT-S Int. Microwave Symp. Dig.*, vol. 3, June 2004, Paper TH-2A-6, pp. 1341–1344.

[5] J. Hilsenbeck, F. Lenk, W. Heinrich, and J. Würfl, "Low phase noise MMIC VCO's for Ka-band applications with improved GaInP/GaAs-HBT technology," in *Proc. IEEE 25th GaAs IC Symp.*, San Diego, CA, Nov. 2003, pp. 223–226.

[6] F. Lenk and M. Rudolph, "New extraction algorithm for GaAs-HBT's with low intrinsic base resistance," in *IEEE MTT-S Int. Microwave Symp. Dig.*, vol. 2, June 2002, pp. 725–728.

[7] J. Hilsenbeck, F. Brunner, F. Lenk, and J. Würfl, "Technology and performance of GaAs/GaInP-HBT MMIC-oscillators for frequencies up to 40 GHz," in *Proc. 26th Compound Semiconductor Devices and Integrated Circuits Workshop*, Moscow, Russia, May 2002, pp. 107–108.

[8] ——, "Fabrication and electrical performance of oscillators in GaAs/GaInP-HBT MMIC technology up to 40 GHz," presented at the 29th Int. Compound Semiconductors Symp., Lausanne, Switzerland, Oct. 2002.

Friedrich Lenk (M'00) was born in Lübbecke/Westfalen, Germany, in 1966. He received the Dipl.-lng. degree in electrical engineering and Dr.-lng. degree from the Technical University of Berlin, Berlin, Germany, in 1995 and 2003, respectively.

He is currently with the Ferdinand-Braun-lnsititut für Höchstfrequenztechnik (FBH), Berlin, Germany. His focus is on modeling and design of MMIC circuits with field-effect transistor (FET) and HBT devices.

Matthias Schott (S'01) was born in Berlin, Germany, in 1974. He received the Dipl.-lng. degree in electrical engineering from the Technical University of Berlin, Berlin, Germany, in 2000.

Since 2000, he has been with the Ferdinand-Braun-lnstitut für Höchstfrequenztechnik (FBH), Berlin, Germany. His focus is on the design of low phase-noise oscillators based on GaAs- and SiGe-based HBT devices.

Jochen Hilsenbeck was born in Laichingen/Alb, Germany, in 1970. He received the Dipl.-lng. degree in electrical engineering from the University of Ulm, Ulm, Germany, in 1996, and the Dr.-lng. degree in GaN-based FETs from the Technical University of Karlsruhe, Karlsruhe, Germany, in 2001.

From 1995 to 1997, he was with the Fraunhofer-lnstitut for Applied Solid State Physics (IAF), Freiburg, Germany. In 1997, he joined the Ferdinand-Braun-lnstitut für Höchstfrequenztechnik (FBH), Berlin, Germany, where he is currently involved with the process technology of HBT-based MMICs in the material systems GaAs and InP.

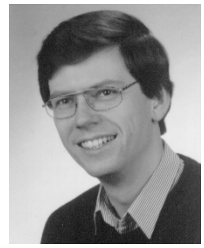

Wolfgang Heinrich (M'84–SM'95) was born in Frankfurt/Main, Germany, in 1958. He received the Dipl.-Ing., Dr.-Ing., and Habilitation degrees from the Technical University of Darmstadt, Darmstadt, Germany, in 1982, 1987, and 1992, respectively.

In 1983, he joined the staff of the lnstitut für Hochfrequenztechnik, Technical University of Darmstadt, where he was involved with the field-theoretical analysis and simulation of planar transmission lines. Since April 1993, he has been with the Ferdinand-Braun-lnstitut für Höchstfrequenztechnik (FBH), Berlin, Germany, where he is Head of the Microwave Department. His current research activities focus on electromagnetic simulation, MMIC design for both GaAs and SiGe, and millimeter-wave packaging.

Dr. Heinrich currently serves as a 2003/2005 Distinguished Microwave Lecturer. He has been chairman of the German IEEE Microwave Theory and Techniques (MTT)/Antennas and Propagation (AP) chapter for the 2002–2005 election periods.